Pkh1/2-dependent phosphorylation of Vps27 regulates ESCRT-I recruitment to endosomes

Joëlle Morvan*, Bruno Rinaldi, and Sylvie Friant
Department of Molecular and Cellular Genetics, Unité Mixte de Recherche 7156, Université de Strasbourg and Centre National de la Recherche Scientifique, 67084 Strasbourg, France

ABSTRACT **Multivesicular endosomes (MVBs) are major sorting platforms for membrane proteins and participate in plasma membrane protein turnover, vacuolar/lysosomal hydrolase delivery, and surface receptor signal attenuation. MVBs undergo unconventional inward budding, which results in the formation of intraluminal vesicles (ILVs). MVB cargo sorting and ILV formation are achieved by the concerted function of endosomal sorting complex required for transport (ESCRT)-0 to ESCRT-III. The ESCRT-0 subunit Vps27 is a key player in this pathway since it recruits the other complexes to endosomes. Here we show that the Pkh1/Phk2 kinases, two yeast orthologues of the 3-phosphoinositide–dependent kinase, phosphorylate directly Vps27 in vivo and in vitro. We identify the phosphorylation site as the serine 613 and demonstrate that this phosphorylation is required for proper Vps27 function. Indeed, in *pkh-ts* temperature-sensitive mutant cells and in cells expressing *vps27*^{S613A}, MVB sorting of the carboxypeptidase Cps1 and of the α-factor receptor Ste2 is affected and the Vps28–green fluorescent protein ESCRT-I subunit is mainly cytoplasmic. We propose that Vps27 phosphorylation by Pkh1/2 kinases regulates the coordinated cascade of ESCRT complex recruitment at the endosomal membrane.**

Monitoring Editor
Judith Klumperman
University Medical Centre Utrecht

Received: Jan 3, 2012
Revised: Jul 2, 2012
Accepted: Aug 15, 2012

INTRODUCTION

The multivesicular endosome (or multivesicular body [MVB]) is a major sorting platform for membrane proteins. The endosomal membrane undergoes an unconventional inward budding, resulting in the formation of intraluminal vesicles, and upon fusion between the MVB and the lysosome/vacuole their content is degraded or matured by resident hydrolases. MVB membrane invagination and protein sorting are achieved by the concerted function of four protein complexes—namely, endosomal sorting complex required for transport (ESCRT)-0 to ESCRT-III. The ESCRT machinery, first discovered in yeast, is highly conserved throughout evolution and is well characterized (Saksena *et al.*, 2007; Williams and Urbe, 2007; Hurley, 2008; Wollert *et al.*, 2009).

The ESCRT-0 complex is composed of vacuolar protein sorting (Vps) 27/hepatocyte growth factor (EGF)-dependent tyrosine kinase substrate (Hrs) and Hbp, STAM, EAST (Hse) 1/signal transducing adaptor molecule (STAM); ESCRT-I of Vps23/tumor suppressor gene 101 (TSG101), Vps28, Vps37, and Mvb12; ESCRT-II of Vps36, Vps22, and Vps25; and ESCRT-III of Vps20, Snf7, Vps24, and Vps2 (Teo *et al.*, 2006; Gill *et al.*, 2007; Obita *et al.*, 2007; Im *et al.*, 2009). The endosomal recruitment of these complexes is sequential and occurs via direct interaction between subunits of two different complexes. The structure of some of these complexes and of the domains important for cargo recognition reveals the interaction interfaces and specific recognition motifs between the complexes (Hierro *et al.*, 2004; Im *et al.*, 2009; Ren *et al.*, 2009; Boura *et al.*, 2011). The disassembly of the complexes is achieved by the catalytic activity of the ATPases associated with various cellular activities (AAA) protein Vps4 and its regulatory subunits Vta1 and Vps60 (Lata *et al.*, 2008).

A key player of these complexes is the ESCRT-0 subunit Vps27/Hrs. It localizes to endosomal membrane through the interaction of

This article was published online ahead of print in MBoC in Press (http://www.molbiolcell.org/cgi/doi/10.1091/mbc.E12-01-0001) on August 23, 2012.

*Present address: Institut de Génétique et de Biologie Moléculaire et Cellulaire, Centre National de la Recherche Scientifique, Unité Mixte de Recherche 7104, Institut National de la Santé et de la Recherche Médicale U 964, 67404 Illkirch Cedex, France.

Address correspondence to: Joëlle Morvan (morvan@igbmc.fr) or Sylvie Friant (s.friant@unistra.fr).

Abbreviations used: CIP, calf intestinal alkaline phophatase; Cps1, carboxypeptidase S; CPY, carboxypeptide Y; ESCRT, endosomal sorting complex required for transport; HA, hemagglutinin; Hrs, hepatocyte growth factor–dependent tyrosine kinase substrate; MVB, multivesicular body; Pkh, Pkb-activating kinase homologue; UEV, ubiquitin E2 variant; Vps, vacuolar protein sorting; Yck, yeast casein kinase; Ypk, yeast protein kinase.

Supplemental Material can be found at:
http://www.molbiolcell.org/content/suppl/2012/08/20/mbc.E12-01-0001.DC1

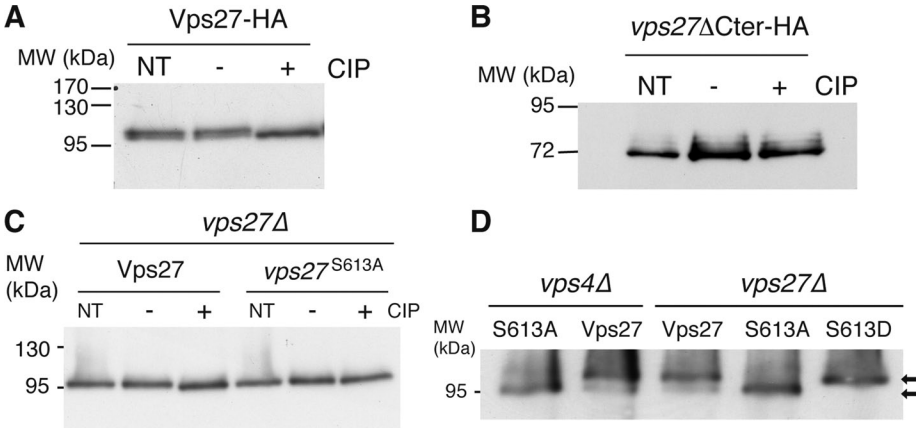

FIGURE 1: Vps27 is a phosphoprotein and is phosphorylated on residue S613 in the C-terminal domain. *vps27*Δ cells transformed with pRS426-Vps27-HA (A), YCpHAC33-*vps27*$^{\Delta Cter}$-HA (B), or YCpHAC33-Vps27 and YCpHAC33-*vps27*^{S613A}-HA (C) total extracts were treated with (+) or without (–) CIP. Samples were analyzed by SDS–PAGE, followed by Western blot using anti-HA antibodies. NT, nontreated. (D) Total extracts of *vps4*Δ or *vps27*Δ cells transformed with pRS426-Vps27-HA, pRS426-vps27^{S613A}-HA, and pRS426-vps27^{S613D}-HA were analyzed by SDS–PAGE, followed by Western blot using anti-HA antibodies.

its Fab1/YOTB1/Vac1/EEA1 (FYVE) domain with phosphatidylinositol 3-phosphate. Vps27/Hrs binds the ubiquitin present on cargoes to be sorted via its ubiquitin-interacting motif (UIM), and it recruits the other complexes to endosomes by direct interaction with the ESCRT-I subunit Vps23/TSG101 (Hurley, 2008). This interaction occurs between the PSDP motifs of Vps27 and the ubiquitin E2 variant (UEV) domain of Vps23 (Pornillos *et al.*, 2002; Katzmann *et al.*, 2003; Ren and Hurley, 2011).

ESCRT-I does not directly interact with the endosomal membrane, and therefore its specific recruitment to endosomes occurs through interaction with ESCRT-0. However, the temporal regulation of ESCRT complex endosomal recruitment and of their association during MVB formation is unclear. Posttranslational modifications of ESCRT subunits by phosphorylation and ubiquitination were suggested to regulate/coordinate their function. In mammalian cells a recent study showed that the ESCRT-0 function is regulated by a kinase interacting with STAM and modulating its ubiquitination status to favor EGF receptor internalization into MVBs (Hanafusa *et al.*, 2011). It was also shown that Hrs is phosphorylated after EGF stimulation, but the role of this modification is under debate, even though it was suggested to be associated with Hrs degradation (Urbe *et al.*, 2000; Stern *et al.*, 2007).

In this study we aim to decipher the role of ESCRT-0 modification by analyzing yeast Vps27/Hrs phosphorylation and identifying the involved kinase. In *Saccharomyces cerevisiae*, only a few kinases involved in the endocytic trafficking pathway have been identified, among them the conserved Pkh-Ypk kinase cascade (Friant *et al.*, 2001; deHart *et al.*, 2002). The Pkh1/2 kinases, the homologues of mammalian 3-phosphoinositide–dependent kinase, are activated by sphingoid bases and phosphorylate the Ypk1 serine–threonine kinase. Ypk1, the homologue of mammalian serum and glucocorticoid–induced kinase, is required for endocytosis but is not necessary for receptor phosphorylation or ubiquitination (deHart *et al.*, 2002). This receptor modification is instead devoted to the yeast casein kinase homologues Yck1 and Yck2, which phosphorylate plasma-membrane proteins, allowing their subsequent ubiquitination and internalization (Hicke *et al.*, 1998; Feng and Davis, 2000; Marchal *et al.*, 2000).

Here we show that phosphorylation of Vps27 is required to regulate ESCRT-0 function. We establish that Vps27 is phosphorylated by the Pkh1/2 kinases on the serine 613 residue. Moreover, we show that this phosphorylation regulates Vps27 cellular functions, as it is necessary for proper endosomal recruitment of ESCRT-I and MVB sorting of cargoes.

RESULTS

Vps27 is phosphorylated on serine 613

The ESCRT cascade needs to be highly regulated for proper endosomal-sorting function. Indeed, in the absence of only one ESCRT subunit, cells accumulate aberrant endosomal structures termed class E compartment, and sorted proteins are blocked in this compartment. Vps27 is a key regulator of this MVB-sorting process, and thus its cellular function most likely requires regulation. Large-scale phosphoproteomic studies identified several phosphorylation sites in Vps27 (Gruhler *et al.*, 2005; Smolka *et al.*, 2007; Albuquerque *et al.*, 2008). Given that phosphorylation/dephosphorylation regulates many important cellular processes, we speculated that Vps27 function could also be regulated by phosphorylation.

To analyze the in vivo phosphorylation status of Vps27, we used a Vps27-hemagglutinin (HA)–tagged protein that rescues the class E compartment phenotype displayed by the *vps27*Δ mutant cells. A total extract of *vps27*Δ cells expressing Vps27-HA was treated with calf intestinal alkaline phosphatase (CIP; Figure 1A). By comparing migration with and without CIP treatment, we observed that upon phosphatase treatment Vps27-HA migrates at a lower molecular weight (Figure 1A), demonstrating that Vps27-HA is phosphorylated in vivo. The C-terminal domain of Vps27 (residues 581–622) is required for ESCRT-I recruitment in vivo (Katzmann *et al.*, 2003). Thus we analyzed the phosphorylation status of a C-terminal–truncated version of Vps27 lacking residues 581–622 (*vps27*$^{\Delta Cter}$). We observed that the migration profile of *vps27*$^{\Delta Cter}$ was unchanged after CIP treatment (Figure 1B). Thus the main Vps27 phosphorylation sites are located in the C-terminal domain.

Based on phosphoproteomics, only one putative phosphorylation site–serine 613–lies in the C-terminal region (581–622) of Vps27 (Gruhler *et al.*, 2005; Smolka *et al.*, 2007; Albuquerque *et al.*, 2008). Thus we generated the vps27^{S613A} mutant by site-directed mutagenesis and analyzed its phosphorylation profile. Total extract of *vps27*Δ transformed by plasmid encoding *vps27*^{S613A}-HA was treated with CIP (Figure 1C). In contrast to the difference observed for wild-type Vps27, the migration profile of *vps27*^{S613A}-HA was not changed after CIP treatment. We also generated point mutants (S155,157A; S274A; S279,280A; S495A; and T497A) for each of the other phosphoresidues identified in Vps27. None of them displayed an altered steady-state phosphorylation profile (Supplemental Figure S1), demonstrating that the phosphorylation of Vps27 occurs predominantly on the S613 residue. Next we generated the phosphomimetic mutant of Vps27, *vps27*^{S613D}-HA and compared its migration profile with that of Vps27-HA and *vps27*^{S613A}-HA in *vps27*Δ (Figure 1D). We observed that *vps27*^{S613D}-HA migrated at the same apparent molecular weight as the wild-type protein, whereas the *vps27*^{S613A}-HA migrated faster. Furthermore, we observed two bands corresponding to Vps27-HA, a more abundant, upper band

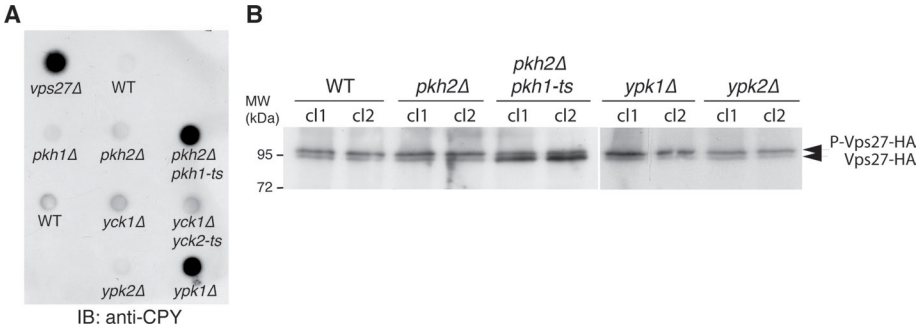

FIGURE 2: The *pkh2*Δ *pkh1-ts* strain displays a defect in CPY sorting and in Vps27 phosphorylation. (A) Wild-type (BY4742), *vps27*Δ, *pkh1*Δ, *pkh2*Δ, *pkh2*Δ *pkh1-ts*, WT (LRB341), *yck1*Δ, *yck1*Δ *yck2-ts ypk2*Δ, and *ypk1*Δ strains were tested for CPY secretion. A 5-µl amount of culture at OD_{600} of 0.4 was spotted on YPD plate and covered with a nitrocellulose membrane. After 48 h of growth at 30°C, CPY was detected using anti-CPY antibodies. (B) Total cell extracts of wild-type, *pkh2*Δ, *pkh2*Δ *pkh1-ts, ypk1*Δ, and *ypk2*Δ strains transformed by pRS426-VPS27-HA were analyzed by SDS–PAGE, followed by Western blot using anti-HA antibodies. Two individual clones were analyzed (cl1 and cl2).

corresponding to the phosphorylated form and a second, minor, lower band corresponding to the unphosphorylated form. This shows that at steady state Vps27 is mainly present in a phosphorylated form. Moreover, a similar profile was observed for Vps27-HA and *vps27*^{S613A}-HA in the *vps4*Δ mutant defective in the disassembly of the ESCRT proteins (Figure 1D), showing that Vps27 is phosphorylated in class E mutant cells. These results indicate that the C-terminal phosphorylation of Vps27 occurs mainly at the S613 residue.

The Pkh kinases are involved in Vps27 phosphorylation

To identify the kinase responsible for Vps27 phosphorylation, we analyzed the kinases required for endocytosis, as MVB sorting and endocytic internalization share common features, such as ubiquitination of the cargo (Lauwers *et al.*, 2010). Only few kinases are involved in endocytosis. Yeast casein kinase I redundant isoforms Yck1 and Yck2 trigger the ubiquitination and internalization of the α-factor receptor Ste2 and of the uracil permease Fur4 (Hicke *et al.*, 1998; Marchal *et al.*, 1998, 2000). Pkh1 and Pkh2, two redundant kinases, act together with their downstream kinases Ypk1 and Ypk2 and are required for the internalization of Ste2 (Friant *et al.*, 2001; deHart *et al.*, 2002).

We hypothesized that posttranslational modifications regulate Vps27 cellular functions, and thus the involved kinase mutant should display similar phenotypes as *vps27*Δ cells. Like all class E *vps* mutants, *vps27*Δ cells mistarget vacuolar hydrolases in the extracellular medium and secrete carboxypeptidase Y (CPY). To analyze the requirement for the redundant kinases in the VPS pathway, we used the temperature-sensitive (ts) *yck1*Δ *yck2-1* and the *pkh2*Δ *pkh1-ts* strains deleted for one isoform and bearing a temperature-sensitive allele of the other isoform (Hicke *et al.*, 1998; Marchal *et al.*, 1998; Friant *et al.*, 2001). The Ypk1 and Ypk2 kinases have redundant essential cellular functions (Chen *et al.*, 1993), but for endocytosis only the *ypk1*Δ cells have an α-factor internalization defect (deHart *et al.*, 2002), and only Ypk1 is phosphorylated and activated by the Pkh kinases (Casamayor *et al.*, 1999). We analyzed the function of the VPS pathway by comparing the CPY secretion displayed by the *yck1*Δ *yck2-1*, *pkh2*Δ *pkh1-ts*, and *ypk1*Δ *ypk2*Δ mutants at 25 and 30°C and used the single mutants *yck2*Δ, *pkh1*Δ, and *pkh2*Δ as controls (Figure 2A). As expected, the wild-type strain did not secrete CPY, in contrast to the *vps27*Δ mutant. At the permissive temperature of 30°C, *pkh2*Δ *pkh1-ts* and *ypk1*Δ strains secreted CPY into the extracellular medium, in contrast to the *yck1*Δ *yck2-ts*, *pkh1*Δ, and *ypk2*Δ mutant strains. This CPY missorting displayed by the *pkh2*Δ *pkh1-ts* strain was more pronounced at 30 than at 25°C and was not restricted to CPY, since on acidic milk plates a clear halo of digestion due to vacuolar hydrolase secretion was also observed (Supplemental Figure S2). Moreover, this mistargeting of vacuolar hydrolases was rescued by the reintroduction of wild-type Pkh2-HA in the *pkh2*Δ *pkh1-ts* mutant and to a lesser extent by the kinase-defective mutant *pkh2*^{K208R} (Supplemental Figure S2). Of interest, the kinase-inactive *pkh2*^{K208R} mutant did not recapitulate the strong *vps* phenotype displayed by the *pkh-ts* cells, suggesting either a partially kinase-independent requirement for this Pkh2 protein or that this kinase mutant is not fully inactive (Inagaki *et al.*, 1999). The *pkh2*^{K208R} mutant is considered as kinase inactive; however, in the initial description and analysis of this mutant, the in vitro phosphorylation assay shows that this mutant had much lower kinase activity than the corresponding wild-type Pkh2 but was not fully inactive (Inagaki *et al.*, 1999). Our results suggest that the Pkh1/2-Ypk1 kinase cascade regulates the VPS pathway.

Because the *pkh2*Δ *pkh1-ts and ypk1*Δ strains displayed a strong CPY secretion phenotype even at the permissive temperature of 30°C, we analyzed Vps27-HA phosphorylation status in these strains. Total extracts from wild-type, *pkh2*Δ, *pkh2*Δ *pkh1-ts*, *ypk1*Δ, and *ypk2*Δ strains transformed with a plasmid encoding for Vps27-HA and grown at 30°C were analyzed (Figure 2B). In *pkh2*Δ, *ypk1*Δ, and *ypk2*Δ mutant cells, as in wild-type cells, Vps27-HA was present as a doublet, with the more abundant, upper band corresponding to the phosphorylated form of Vps27-HA. In contrast, in the *pkh2*Δ *pkh1-ts* strain, the upper band signal was strongly decreased compared with that of the lower band, indicating that Vps27-HA phosphorylation was impaired in this mutant. This result demonstrates that Pkh1/2 are required for proper steady-state phosphorylation of Vps27 in vivo.

Pkh2 phosphorylates Vps27 at the S613 residue in vitro

To investigate whether Pkh2 directly phosphorylates Vps27, we performed an in vitro phosphorylation assay. Purified recombinant hexahistidine (6xHis)-Vps27 produced in *Escherichia coli* thus made void of posttranslational modifications was incubated with Pkh2-HA or kinase-inactive *pkh2*^{K208R}-HA immunoisolated from *pkh1*Δ cells (Supplemental Figure S3) in the presence of [γ-^{32}P]ATP. The Pkh2-HA construct was active, as it rescued the temperature-sensitive growth and the vacuolar hydrolases secretion of the *pkh2*Δ *pkh1-ts* strain, and a similar complementation was observed for the kinase-inactive *pkh2*^{K208R}-HA construct, albeit to a lesser extent than for the wild-type Pkh2 (Supplemental Figure S2).

We observed a weak band corresponding to ^{32}P-labeled 6xHis-Vps27 in the absence of Pkh2-HA (Figure 3A, lane 2). On addition of Pkh2-HA beads to the phosphorylation mix a strong signal for the high–molecular weight band corresponding to Pkh2 autophosphorylation was observed (Figure 3A, lane 3). This shows that the kinase is active in our in vitro assay. Incubation of the Pkh2-HA kinase with 6xHis-Vps27 induced Vps27 phosphorylation (Figure 3A, lane 4), compared with the weaker signal observed in absence of the kinase (Figure 3A, lane 2). In contrast, in the presence of the kinase-inactive mutant *pkh2*^{K208R} (Figure 3A, lane 6), the signal corresponding to

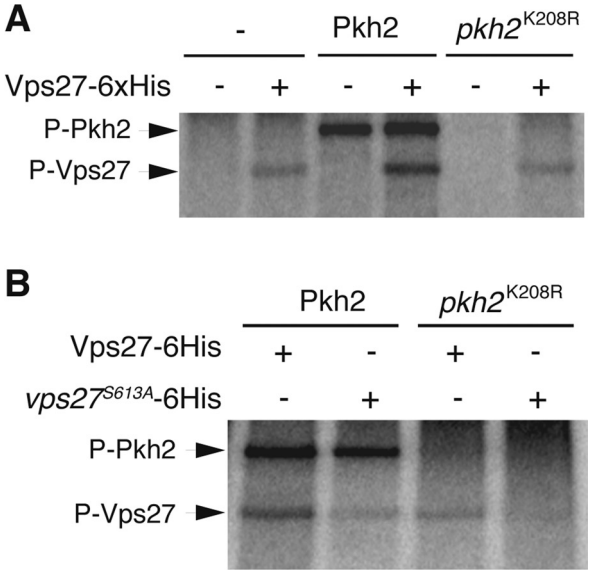

FIGURE 3: Pkh2 phosphorylates directly Vps27 on residue S613 in vitro. Anti-HA immunoprecipitation was performed from total lysate of *pkh1*Δ cells transformed with empty plasmid or wild-type or kinase-inactive (K208R) Pkh2-HA–encoding plasmid. Beads were used in an in vitro phosphorylation assay with 25 µg of recombinant Vps27-6xHis (A, B) or vps27^{S613A}-6xHis (B) in the presence of [γ-^{32}P]ATP. Samples were analyzed by SDS–PAGE, and the gels were dried and exposed for 24 h on a phosphoscreen. A representative experiment is shown; the experiment was repeated at least three times.

phosphorylated 6xHis-Vps27 was similar to the background level (Figure 3A lane 2). In addition, no autophosphorylation of this *pkh2*^{K208R} kinase-inactive mutant was detected, ensuring that the mutation altered the kinase activity of the protein. These results demonstrate that Pkh2 directly phosphorylates Vps27 in vitro.

We next asked whether the S613 residue was the target of Vps27 phosphorylation by Pkh2. We purified the 6xHis-*vps27*^{S613A} recombinant protein from *E. coli* (Supplemental Figure S3A). 6xHis-tagged Vps27 and *vps27*^{S613A} were subjected to in vitro phosphorylation by Pkh2-HA or *pkh2*^{K208R}-HA immunoprecipitated from *pkh1*Δ cells (Figure 3B). In contrast to Vps27, which was phosphorylated by Pkh2, *vps27*^{S613A} phosphorylation strongly decreased. In the presence of the kinase-inactive *pkh2*^{K208R}, the residual phosphorylation observed for Vps27 also decreased for *vps27*^{S613A} (Figure 3B). This result demonstrates that the S613 residue is specifically required for Pkh2-dependent phosphorylation of Vps27 in vitro.

Vps27 phosphorylation is required for cargo sorting at the MVB

Vps27 fails to be properly phosphorylated in *pkh2*Δ *pkh1-ts* cells, and thus we investigated whether this affected its MVB-sorting function. We analyzed the trafficking of the carboxypeptidase S Cps1–green fluorescent protein (GFP), which is normally sorted in a ubiquitin-dependent manner into MVB intralumenal vesicles and then delivered to the vacuolar lumen (Reggiori and Pelham, 2001). Wild-type, *pkh2*Δ, and *pkh2*Δ *pkh1-ts* cells transformed with a plasmid encoding Cps1-GFP were grown at 30°C and observed for fluorescence. In wild-type and *pkh2*Δ cells, Cps1-GFP was localized to the vacuolar lumen (Figure 4A). In contrast, in *pkh2*Δ *pkh1-ts* cells Cps1-GFP was mislocalized at the vacuolar membrane, showing that the Pkh1/2 kinases are required for proper MVB sorting.

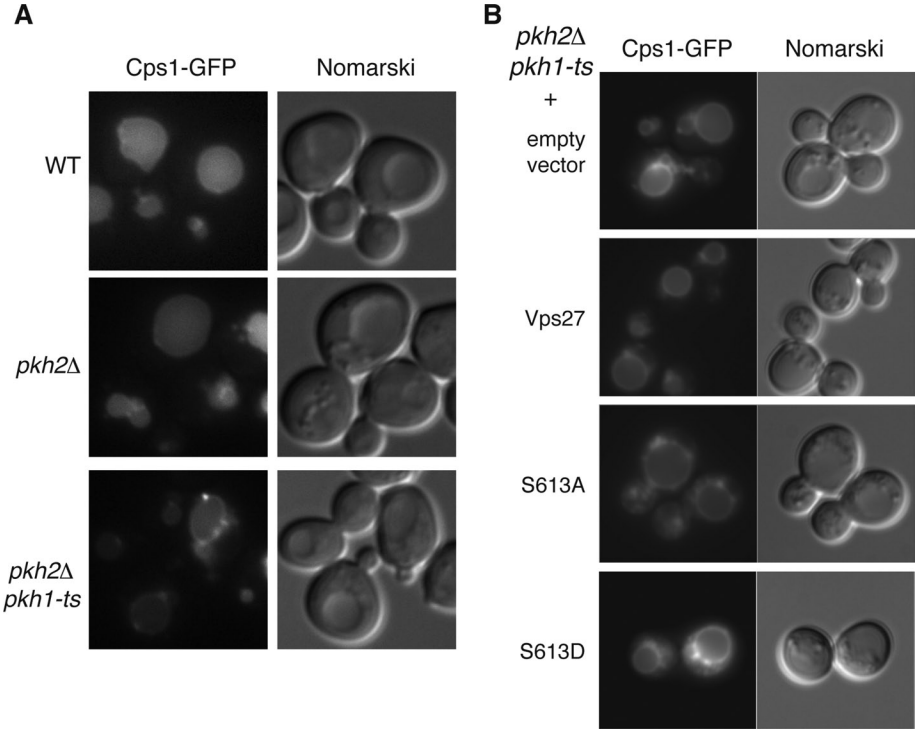

FIGURE 4: Pkh1/2 kinases are required for MVB sorting. (A) Wild-type, pkh2Δ, and *pkh2*Δ *pkh1-ts* strains transformed with Cps1-GFP (pGO45) were grown at 30°C until exponential phase and observed by fluorescence microscopy. (B) *pkh2*Δ *pkh1-ts* cells cotransformed with Cps1-GFP (pGO47) and empty plasmid (YCpHAC33), YCpHAC33-Vps27-HA, YCpHAC33-vps27$^{\Delta Cter}$-HA, YCpHAC33-vps27^{S613A}-HA, or YCpHAC33-vps27^{S613D}-HA were grown at 30°C until exponential phase and observed by fluorescence microscopy.

Because Pkh1/2 kinases phosphorylate Vps27 and are required for endosomal sorting, we addressed the subcellular localization of Pkh2. We used wild-type and class E *vps4*Δ mutant cells bearing *PKH2* tagged at the locus with GFP and observed the localization of Pkh2-GFP by fluorescence microscopy (Supplemental Figure S4A). In both strains, Pkh2-GFP localized mainly to punctae near the plasma membrane and in one or few intracellular dots that did not colocalize with the class E compartment in *vps4*Δ cells. This shows that the Pkh kinases are not clustered in the aberrant class E endosomal compartment. We also analyzed the subcellular distribution of Pkh2-GFP in wild-type and *vps4*Δ strains (Supplemental Figure S4B). Whole-cell lysates (T) were subjected to differential centrifugation to generate two membrane fractions—the 13,000 × *g* pellet (P13) and the 100,000 × *g* pellet (P100)—and a cytosolic fraction—the 100,000 × *g* supernatant (S100). The proper fractionation was attested by the presence in P13 and P100 of the soluble *N*-ethylmaleimide–sensitive factor attachment protein receptor Vti1 that cycles between Golgi and endosomal membranes, in P13 of the vacuolar membrane alkaline phosphatase (ALP), and in S100 of the cytosolic

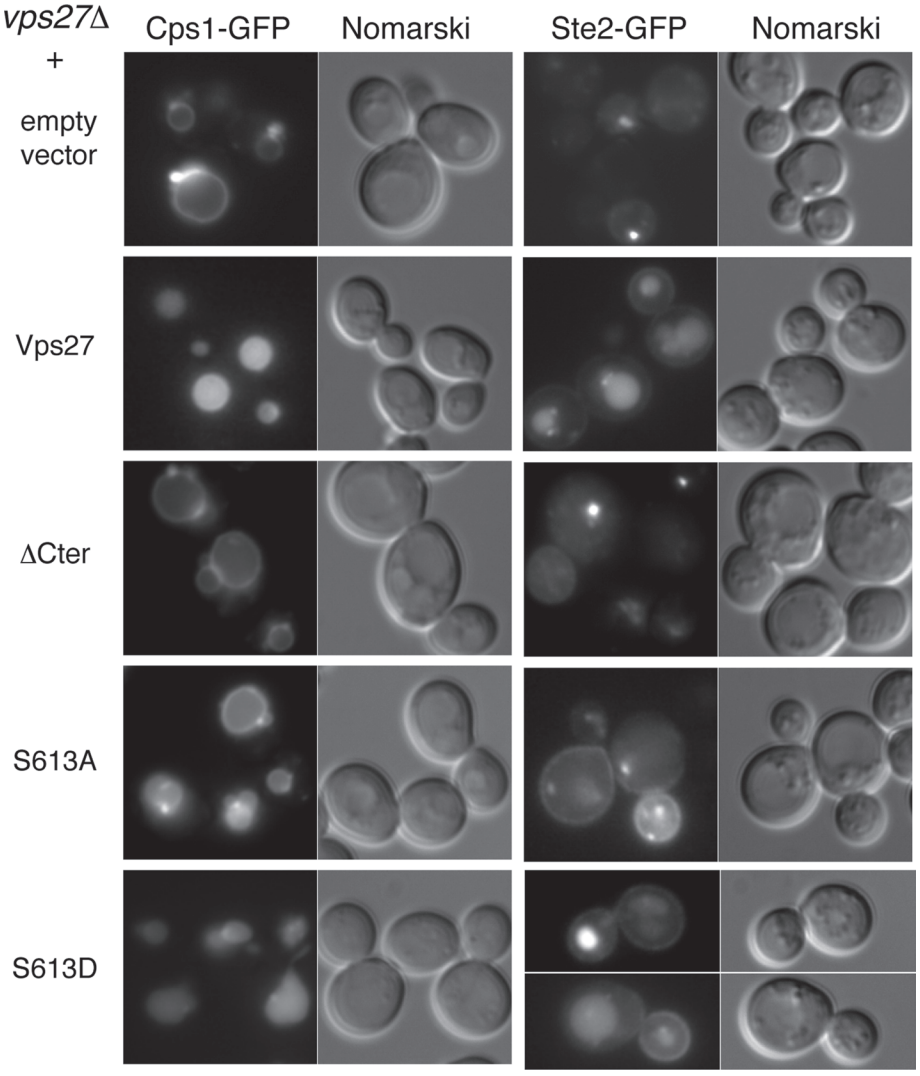

FIGURE 5: Vps27 phosphorylation on Ser613 is required for proper MVB sorting. The vps27Δ cells cotransformed with Cps1-GFP (pGO47) or Ste2-GFP and empty plasmid (YCpHAC33), YCpHAC33-Vps27-HA, YCpHAC33-vps27$^{\Delta Cter}$-HA, YCpHAC33-vps27^{S613A}-HA, or YCpHAC33-vps27^{S613D}-HA were grown at 30°C until exponential phase and observed by fluorescence microscopy.

phospho–glycerate kinase Pgk1 (Supplemental Figure S4B). Pkh2-GFP was mainly detected in membrane fractions (P13 and P100) in both wild-type and *vps4*Δ cells. These data show that Pkh2-GFP is associated with plasma membrane and intracellular membranes but is not enriched in endosomes. We also performed a subcellular fractionation of Pkh2-HA in wild-type cells and observed the same distribution as with Pkh2-GFP (Supplemental Figure S4B), demonstrating that the overproduction or the nature of the tag did not change the subcellular localization of the protein.

To decipher the role of the S613 residue in the MVB-sorting function of Vps27, we analyzed the localization of the vacuolar protein Cps1-GFP in *vps27*Δ cells transformed with empty plasmid or plasmid encoding HA-tagged Vps27, *vps27*^{S613A}, or *vps27*^{S613D} (Figure 5). As expected, in the *vps27*Δ cells transformed with empty plasmid and HA-tagged *vps27*$^{\Delta Cter}$, Cps1-GFP was retained in the class E compartment and at the vacuolar membrane. In *vps27*Δ cells expressing *vps27*^{S613A}-HA, Cps1-GFP was missorted at the vacuolar membrane but was also found in the vacuolar lumen. In contrast, in *vps27*Δ cells expressing wild-type Vps27-HA or the phosphomimetic *vps27*^{S613D}-HA mutant, Cps1-GFP was properly localized to the vacuolar lumen. We also analyzed the vacuolar delivery of the α-factor receptor Ste2, which follows the endocytic pathway and is internalized in the intraluminal vesicles of MVBs before its delivery and degradation into the vacuolar lumen (Stefan and Blumer, 1999). In the *vps27*Δ cells bearing the empty vector or the *vps27*$^{\Delta Cter}$ construct, Ste2-GFP accumulated in the class E compartment, and this accumulation was also observed for the *vps27*^{S613A} mutant but to a lesser extent, whereas in the presence of wild-type Vps27 or of the phosphomimetic *vps27*^{S613D} mutant, Ste2-GFP was properly delivered into the lumen of the vacuole (Figure 5). These results show that the phosphorylation of Vps27 on S613 is required for proper MVB sorting of cargo proteins.

It is striking that the phosphomimetic *vps27*^{S613D} mutant complemented the CPY secretion defect displayed by the *vps27*Δ cells, whereas the *vps27*^{S613A} mutant showed only a partial rescue (Supplemental Figure S2C). We thus wondered whether the phosphomimetic *vps27*^{S613D} mutant could complement the VPS defect displayed by the *pkh2*Δ *pkh1-ts* cells. We analyzed the MVB sorting of Cps1-GFP in the *pkh2*Δ *pkh1-ts* cells bearing the empty vector, the Vps27 WT or the *vps27*^{S613A} or *vps27*^{S613D} mutant at 30°C (Figure 4B). None of the Vps27 variants rescued the Cps1-GFP mislocalization at the vacuolar membrane in the *pkh2*Δ *pkh1-ts* cells. We also observed that neither the temperature sensitivity nor the secretion of CPY displayed by the *pkh2*Δ *pkh1-ts* cells were rescued by the expression of Vps27, *vps27*^{S613A}, or *vps27*^{S613D} (Supplemental Figure S2C). These results suggest that Vps27 is not the only effector of the Pkh kinase involved in MVB sorting.

To rule out that Vps27 mutants are not properly localized, we subjected *vps27*Δ cells transformed with empty plasmid or plasmid encoding HA-tagged Vps27, *vps27*^{S613A}, or *vps27*^{S613D} to subcellular fractionation (Supplemental Figure S5A). Whole-cell lysates (T) were subjected to differential centrifugation to generate the P13 and P100 membrane fractions and the S100 cytosolic fraction. Equal volumes of the fractions were analyzed by Western blot using anti-HA antibody and antibodies directed against control proteins (Vps10 and Pgk1). The proper fractionation was attested by the presence of the Vps10 transmembrane receptor, which cycles between Golgi and endosomes in P13 and P100 and of Pgk1 in S100. Wild-type, S613A, and S613D Vps27 were all found mostly in the P13 and P100 fractions and to a lesser extent in the S100 fraction. Thus mutation of the S613 residue does not alter Vps27 membrane localization.

Vps27 phosphorylation is required for Vps28-GFP recruitment to endosomes

We hypothesized that Pkh2-dependent phosphorylation of Vps27 in the C-terminal domain might regulate the interaction with

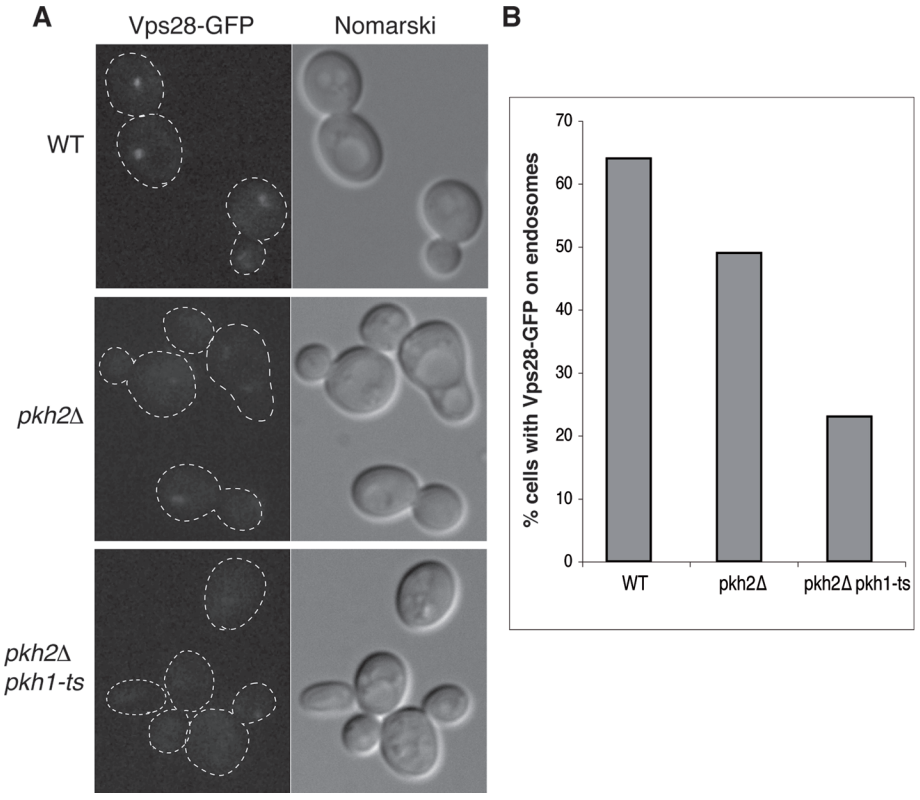

FIGURE 6: Vps28-GFP is not properly recruited to endosomes in the *pkh2Δ pkh1-ts* mutant. (A) Wild-type, *pkh2Δ*, and *pkh2Δ pkh1-ts* strains bearing GFP-tagged Vps28 under its own promoter were grown until exponential phase of growth at 25°C. Cells were then imaged by fluorescence microscopy. (B) Quantification was made on two independent clones and >200 cells.

ESCRT-I and thus its recruitment to endosomes. The ESCRT-I complex, composed of Vps23, Vps28, Vps37, and Mvb12, assembles in the cytoplasm and is recruited to the endosomal membrane via direct binding between Vps27 and Vps23 (Pornillos *et al.*, 2002; Katzmann *et al.*, 2003; Ren and Hurley, 2011). Thus we analyzed whether the phosphorylation of Vps27 on the S613 residue was required for its direct interaction with Vps23. Pull-down studies revealed that Vps23-GFP interacted to the same extent with wild-type, S613A, or S613D Vps27-6His recombinant proteins immobilized on nickel-nitriloacetic acid beads (Supplemental Figure S5B). We confirmed these results by performing coimmunoprecipitation of HA-tagged Vps27, $vps27^{S613A}$, and $vps27^{S613D}$ with Vps23-GFP from *vps27Δ* cells (Supplemental Figure S5C). Vps23-GFP was able to coimmunorecipitate Vps27, as well as the $vps27^{S613A}$ and $vps27^{S613D}$ variants. Thus the Cps1-sorting defect displayed by cells expressing the $vps27^{S613A}$ mutant is not due to a lack of interaction with Vps23. It was previously shown that Vps27 lacking its C-terminal domain (Δ581–622) is able to interact with Vps23 (Bilodeau *et al.*, 2003) but is defective for Cps1 MVB sorting and fails to recruit the ESCRT-I subunit Vps23 on endosomes (Katzmann *et al.*, 2003). Therefore, we analyzed the endosomal recruitment of the ESCRT-I subunit Vps28-GFP in wild-type, *pkh2Δ*, and *pkh2Δ pkh1-ts* cells (Figure 6). The GFP tag did not induce Vps28 misfunction, since the cells showed normal vacuoles and no class E phenotypes (unpublished data). In the wild-type parental strain as well as in the *pkh2Δ* cells, Vps28-GFP localized to a large punctuate structure juxtaposed to the vacuole corresponding to the endosomes. In contrast, in *pkh2Δ pkh1-ts* cells at permissive temperature (30°C), Vps28-GFP was mainly localized to the cytoplasm as a diffuse fluorescence in most of the cells (77%; Figure 6). To ensure that this mislocalization of Vps28-GFP was not due to a mislocalization of Vps27, we also analyzed the localization of Vps27 tagged at the locus with GFP in the wild-type, *pkh2Δ*, and *pkh2Δ pkh1-ts* cells (Supplemental Figure S6). Vps27-GFP was detected as large punctae juxtaposed to the vacuole and corresponding to endosomes in all these strains. These results strongly suggest that Pkh1/2 kinases regulate ESCRT-I recruitment to endosomes.

Next we investigated whether the phosphorylation of Vps27 at residue S613 was required for the recruitment of Vps28 to endosomes. We thus analyzed the localization of chromosomally tagged Vps28-GFP in *vps27Δ* cells transformed with empty plasmid or plasmid encoding HA-tagged Vps27, $vps27^{\Delta Cter}$, $vps27^{S613A}$, or $vps27^{S613D}$ (Figure 7). As expected, in *vps27Δ* cells transformed with the empty plasmid, GFP-Vps28 was cytosolic. A normal localization at the endosomes was restored in the presence of Vps27-HA, showing that Vps27-HA efficiently recruits ESCRT-I. As previously described (Katzmann *et al.*, 2003), we observed that the $vps27^{\Delta Cter}$-HA construct did not allow the recruitment of Vps28-GFP at the endosomes. In *vps27Δ* cells transformed with $vps27^{S613A}$-HA, Vps28-GFP displayed also mostly a cytoplasmic localization (80% of cells); in contrast, the phosphomimetic mutant $vps27^{S613D}$-HA exhibited increased endosomal localization of Vps28-GFP, even if this rescue was not as efficient as the one observed for the wild-type Vps27 (Figure 7B). It was previously shown that in the *vps4Δ* class E mutant cells impaired in ESCRT dissociation from endosomes, the $vps27^{\Delta Cter}$ mutant was not defective for Vps23 recruitment on endosomes (Katzmann *et al.*, 2003). Therefore, we also analyzed the endosomal recruitment of Vps28-GFP in the *vps4Δ vps27Δ* cells expressing Vps27, $vps27^{S613A}$, or $vps27^{S613D}$ (Supplemental Figure S7). In the *vps4Δ* class E mutant cells, Vps28-GFP endosomal recruitment was restored for $vps27^{S613A}$ mutant and ameliorated for the $vps27^{S613D}$ mutant. This confirmed that the S613 residue was not required for the interaction of Vps27 with Vps23. These results demonstrate that the S613 residue is required for the proper recruitment of Vps28-GFP to endosomes. Taken together, these results show that phosphorylation of the residue S613 of Vps27 and the presence of Pkh1/2 kinases are required for the endosomal recruitment of the ESCRT-I complex. We propose that the phosphorylation status of Vps27 regulates its ESCRT-I recruitment function and thus the coordinated function of the ESCRT complexes.

DISCUSSION

In this study we report that Vps27 is mainly found in a phosphorylated form in vivo and that this phosphorylation occurs in the C-terminal domain of the protein. By screening kinases involved in endocytosis for a general defect in the VPS pathway, we identified Pkh1/2 as the kinases phosphorylating Vps27. In addition, we demonstrated that Pkh1/2 phosphorylates Vps27 in vivo and in vitro. We identified the serine 613 as critical for proper phosphorylation of Vps27 in vivo and as the target of Pkh2 phosphorylation in vitro. Moreover, Vps27

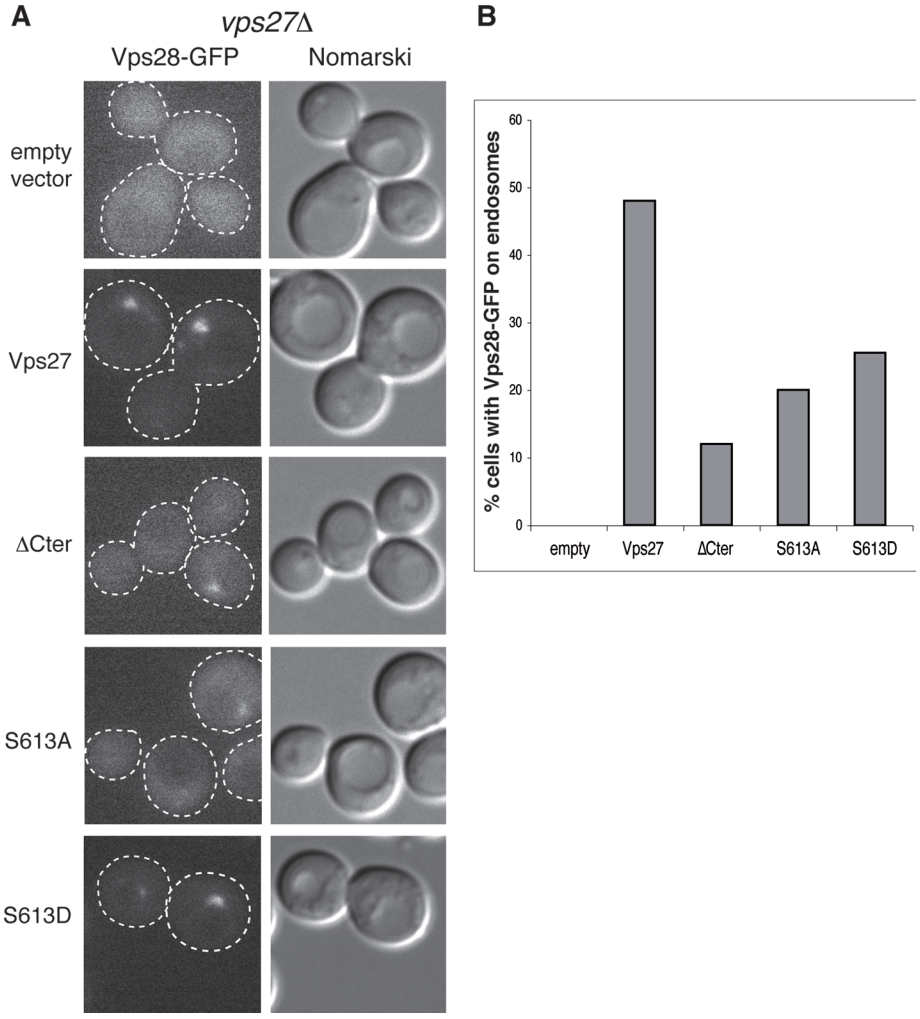

FIGURE 7: Vps28-GFP is not properly recruited to endosomes in cells producing Vps27 lacking its C-terminal domain or bearing the S613A mutation. (A) The *vps27*Δ vps28-GFP strain was transformed with empty plasmid (YCpHAC33) or YCpHAC33 plasmid encoding wild-type, ΔCter, S613A, or S613D Vps27-HA. Cells were grown until exponential phase of growth at 25°C and imaged by fluorescence microscopy. (B) Quantification was made on two independent clones and >200 cells.

phosphorylation is required for MVB sorting of cargo like Cps1 and Ste2, a missorting most likely due to the impaired recruitment of ESCRT-I to endosomes. Indeed in a *pkh2*Δ *pkh1-ts* mutant, the ESCRT-I subunit Vps28 is partly mislocalized to the cytoplasm. This defect is also observed in cells bearing *vps27*^{S613A} as the sole source of Vps27. Thus Vps27 phosphorylation by Pkh1/2 on serine 613 regulates the recruitment of ESCRT-I to endosomes.

In *S. cerevisiae* endocytosis is dependent on sphingoid base (Zanolari *et al.*, 2000). It was shown that Pkh1/2 kinases are activated by sphingoid base and are required for the internalization step of endocytosis (Friant *et al.*, 2001). The overexpression of these kinases can restore endocytosis in the *lcb1-100* mutant deficient in sphingolipid synthesis. Here we show that in addition to its role in the early step of endocytosis, Pkh2 also displays a general defect in the VPS pathway and can directly phosphorylate Vps27 to regulate ESCRT-I recruitment to endosomes. Thus Pkh1/2 kinases also play an important role at a later stage of endocytosis. Consistent with the observation of Marchal *et al.* (2001), we showed that the *yck1*Δ *yck2-ts* mutant did not display a general VPS pathway defect (Figure 2). Of interest, it was recently shown that Yck2 is palmitoylated, leading to its anchorage at the plasma membrane (Roth *et al.*, 2011). This plasma-membrane specific localization of Yck2 might explain why it cannot act directly at later stage of endocytosis. In contrast, we showed that the *pkh2*Δ *pkh1-ts* mutant displays a strong secretion of vacuolar hydrolases, attesting to a general VPS pathway defect (Figure 2 and Supplemental Figure S2) and that this defect was not restored by the phosphomimetic *vps27*^{S613D} mutant (Supplemental Figure S2 and Figure 4B), suggesting that Vps27 was not the only Pkh1/2 effector. Furthermore, we showed that *ypk1*Δ mutant displays a CPY secretion phenotype (Figure 2), suggesting that the Pkh1/2 kinases could also act on its downstream effector Ypk1 to regulate the vacuolar sorting of hydrolases. The Pkh1/2 kinases might also act as a protein platform to regulate the trafficking function of some additional effector(s) via protein–protein interactions, as the *pkh2*^{K208R} mutant that is considered as kinase inactive did not recapitulate the strong VPS defect displayed by the *pkh2*Δ *pkh1-ts* mutant cells.

Vps27 binds directly to the UEV domain of the ESCRT-I subunit Vps23 and recruits the whole complex to endosomes. It was shown by pull-down experiments with recombinant GST fusion of a truncated version of Vps27 that residues 431–485, including the ^{447}PSDP^{450}-1 and ^{523}PSDP^{536}-2 motifs of Vps27, were required for interaction with the UEV domain of Vps23 (Bilodeau *et al.*, 2003). However, Katzmann *et al.* (2003) showed that the residues 581–622 and the ^{581}PTVP^{584} motif of Vps27 control Vps23 endosomal localization in vivo. Of interest, recent interaction and structural studies confirmed the interaction between the PDSP motifs of Vps27 and an N-terminal motif on the UEV domain of Vps23 (Ren and Hurley, 2011). However, this interaction motif was not essential for the MVB sorting of Cps1 (Ren and Hurley, 2011). Here we show that the S613 residue in the C-terminal domain of Vps27 (581–622) is required to trigger the recruitment of the whole ESCRT-I complex to endosomes, as Vps28-GFP was mislocalized in its absence. Moreover, the single mutation of the phosphorylation site S613 is sufficient to alter the recruitment of the ESCRT-I complex by Vps27, and this without altering the capacity of Vps27 to bind to Vps23 (Supplemental Figure S5, B and C). We hypothesize that the function of this phosphorylation is to regulate the recruitment of ESCRT-I, perhaps by facilitating the accessibility to the PSDP motifs. In mammalian cells the Vps27 homologue Hrs is phosphorylated on residue Y334, which is just upstream of the ^{348}PSAP^{351} motif required for TSG101 interaction, upon EGF stimulation (Urbe *et al.*, 2000; Steen *et al.*, 2002). These observations allow us to speculate that Hrs–TSG101 interaction might also be modulated by phosphorylation. The role of Hrs phosphorylation remains unclear; it was suggested that it triggers relocation of Hrs from cytosol to endosome (Urbe *et al.*, 2000), but was also described as responsible for Hrs cytosolic relocation and degradation (Stern *et al.*, 2007). Using subcellular fractionation, we

observed no major differences in Vps27 distribution upon mutation of the S613 residue, suggesting that the phosphorylation of this residue does not alter Vps27 endosomal localization (Supplemental Figure S5A). An explanation for the importance of Hrs phosphorylation in ESCRT-I recruitment to endosomes is that phosphorylation of a residue lying next to the P(T/S)AP motifs might trigger a conformational change resulting in better accessibility of this motif to ESCRT-I (TSG101/Vps23) binding.

Several other residues of Vps27 can be phosphorylated (Gruhler *et al.*, 2005; Smolka *et al.*, 2007; Albuquerque *et al.*, 2008). We analyzed the steady-state phosphorylation status of point mutants of these residues (S155,157A; S274A; S279,280A; S495A; and T497A) and found none required for steady-state phosphorylation of Vps27 (Supplemental Figure S1). However, this does not exclude a role in regulating Vps27 cellular functions and thus the MVB pathway in different environmental or stress conditions. Indeed, two of these residues, S157 and S495, in the FYVE and C-terminal region, respectively, are hyperphosphorylated upon α-factor treatment (Gruhler *et al.*, 2005). It will be interesting to further investigate the role of the phosphorylation of these residues and to identify the kinases involved in these modifications.

In the ubiquitin-binding domain containing protein, ubiquitination is involved in intramolecular inhibition of the ubiquitin binding (Hoeller *et al.*, 2006). Phosphorylation can regulate ubiquitination of proteins; for example, in the case of the uracil permease Fur4 phosphorylation of the PEST sequence is required for proper ubiquitination and subsequent internalization of the protein (Marchal *et al.*, 2000). Thus phosphorylation could also regulate the ubiquitination of Vps27 and thus its ability to bind ubiquitinated cargoes. It has been shown that the ESCRT-0 protein STAM (Hse1 in yeast) ubiquitination is increased upon down-regulation of the scaffold leucine-rich repeat kinase LRRK1, and this regulates endosomal trafficking of the EGF receptor (Hanafusa *et al.*, 2011). Thus a similar mechanism could exist for the regulation of Vps27 ubiquitin binding via its UIM motif. It will be important to further characterize the role of the phosphorylation of the different residues of Vps27.

Phosphorylation of Vps27 at residue S613 is important for the regulation of ESCRT function, and thus the dephosphorylation step must also play an important role in this process. One protein phosphatase candidate is the phosphatase 2A (PP2A). Indeed, Friant *et al.* (2000) showed that its loss of activity, as well as Pkc1 overexpression, can suppress sphingoid base requirement for endocytosis. This suggests that PP2A acts in the same pathway as Pkh1/2 to regulate endocytosis. Further investigations should be carried out to decipher the role of this phosphatase in the regulation of MVB function.

In conclusion, we showed that phosphorylation of Vps27 is crucial for endosomal recruitment of the ESCRT machinery and thus required for proper MVB sorting, which gives new insight into the regulation of the ESCRT machinery assembly. Considering the high degree of conservation of the MVB pathway throughout evolution, we propose that this might be a conserved regulatory mechanism of MVB function.

MATERIALS AND METHODS

Strains, plasmids, media, and growth conditions

Yeast strains and plasmids used in this study are listed in Tables 1 and 2, respectively. Yeast strains were transformed using a modified version of the lithium acetate method (Gietz *et al.*, 1992).

Cells were grown at 30°C or at the indicated temperature in rich medium (YPD; 1% yeast extract, 2% peptone, 2% glucose) or synthetic medium (SC; 0.67% yeast nitrogen base without amino

Name	Genotype	Origin
BY4742	Mat α *his3Δ1 leu2Δ0 lys2Δ0 ura3Δ0*	EUROSCARF
VPS27Δ	Mat α *his3Δ1 leu2Δ0 lys2Δ0 ura3Δ0 vps27*::KanMX4	EUROSCARF
SFY105	Mat α *his3Δ1 leu2Δ0 lys2Δ0 ura3Δ0 trp1::hphMX4 vps27*::KanMX4	This study
YPK1Δ	Mat α *his3Δ1 leu2Δ0 lys2Δ0 ura3Δ0 ypk1*::KanMX4	EUROSCARF
YPK2Δ	Mat α *his3Δ1 leu2Δ0 lys2Δ0 ura3Δ0 ypk2*::KanMX4	EUROSCARF
LRB341	Mat α *his3 leu2 ura3-52*	Robinson *et al.* (1993)
LRB343	Mat α *his3 leu2 ura3-52 yck2-1::HIS3*	Robinson *et al.* (1993)
LRB346	Mat α *his3 leu2 ura3-52 yck1Δ yck2-1*	Robinson *et al.* (1993)
INA17-4D	Mat a *ura3 trp1 leu2 his2 ade1*	Inagaki *et al.* (1999)
RH5413	Mat a *ura3-52 trp1-1 leu2-3112 his2 ade2 lys2 bar1::URA3 pkh1::TRP1*	Friant *et al.* (2001)
RH5388	Mat a *ura3 trp1 leu2 his2 ade2 pkh2::LEU2*	Friant *et al.* (2001)
INA106-3D	Mat α *ura3 trp1 leu2 his2 ade1 pkh2::LEU2 pkh1-ts*	Inagaki *et al.* (1999)
SFY104	Mat a *ura3 leu2 his2*	This study
SFY103	Mat a *ura3 his pkh2::LEU2*	This study
SFY102	Mat α *ura3 his met15 pkh2::LEU2 pkh1-ts*	This study
SFY93	Mat a *ura3 leu2 lys2 vps27::KanMX VPS28-GFP::HIS3*	This study
SFY97	Mat α *ura3 trp1 met15 pkh2::LEU2 pkh1-ts VPS28-GFP::HIS3*	This study
SFY98	Mat a *ura3 trp1 met15 pkh2::LEU2 VPS28-GFP::HIS3*	This study
SFY99	Mat α *ura3 leu2 VPS28-GFP::HIS3*	This study
Pkh2-GFP	Mat a *his3Δ1 leu2Δ0 met15 ura3Δ0 PKH2-GFP::HIS3*	EUROSCARF
SFY133	Mat α *his3Δ1 leu2Δ0 lys2Δ0 ura3Δ0 PKH2-GFP::HIS3 vps4*::KanMX4	This study
SFY136	*his3Δ1 leu2Δ0 lys2Δ0 ura3Δ0 PKH2-GFP::HIS3 vps27:: KanMX vps4*::KanMX4	This study
Vps27-GFP	Mat a *his3Δ1 leu2Δ0 met15 ura3Δ0 VPS27-GFP::HIS3*	EUROSCARF
SFY95	Mat a *his3 leu2 ura3 VPS27-GFP::HIS3 pkh2::LEU2 pkh1-ts*	This study
SFY96	Mat a *his3 leu2 ura3 met15 VPS27-GFP::HIS3 pkh2::LEU2*	This study

TABLE 1: Yeast strains.

Name	Description	Origin
pTS81	YEp195-*PKH2*-3xHA, URA3, 2 μm	T. Schmelzle and M. N. Hall, University of Basel, Switzerland
pSF55	YEp195-*pkh2^{K208R}-3xHA, URA3, 2 μm*	This study
pDL56	pRS426-Prom-*VPS27*-3xHA, *URA3, 2 μm*	R. C. Piper, University of Iowa
pSF51	YCpHAC33-Prom-*VPS27*-3xHA, *URA3, CEN*	This study
pSF52	YCpHAC33-Prom-*vps27$^{\Delta Cter}$*-3xHA, *URA3, CEN*	This study
pSF65	YCpHAC33-Prom-*vps-27^{S613A}*-3xHA, *URA3, CEN*	This study
pSF68	YCpHAC33-Prom-*vps27^{S613D}*-3xHA, *URA3, CEN*	This study
pSF69	pRS426- Prom-*vps27^{S613A}*-3xHA, *URA3, 2* μm	This study
pSF70	pRS426- Prom-*vps27^{S613D}*-3xHA, *URA3, 2* μm	This study
pDB17	pET15b-6xHis-*VPS27, Amp, Ori*	This study
pSF66	pET15b-6xHis-*vps27^{S613A}, Amp, Ori*	This study
pSF71	pET15b-6xHis-*vps27^{S613D}, Amp, Ori*	This study
pGO45	pRS426-GFP-Cps1, *URA3, 2* μm	Odorizzi *et al*. (1998)
pGO47	pRS424-GFP-Cps1, *TRP1, 2* μm	Odorizzi *et al*. (1998)
pSte2-GFP	pRS424-Ste2-GFP, *TRP1, 2* μm	Stefan and Blumer (1999)
pJMG282	pRS415-prom ADH-GFP-VPS23, *LEU2, CEN*	Bugnicourt *et al*. (2004)

TABLE 2: Plasmids.

acids, 2% glucose, and the appropriate CSM [MP Biomedicals, Solon, OH] dropout mix).

The SFY93, SFY97, SFY98, SFY99, SFY102, SFY103, and SFY104 strains were obtained by crossing BY4741 *VPS28-GFP* (European *Saccharomyces cerevisiae* Archive for Functional Analysis [EUROSCARF], Institute for Molecular Biosciences, Johann Wolfgang Goethe-University Frankfurt, Frankfurt, Germany) with INA106-3D. The SFY93 strain was obtained by crossing the BY4742 *vps27*Δ strain with the BY4741 *VPS28-GFP* strain. The SFY133 strain was obtained by crossing BY4742 *vps4*Δ (EUROSCARF) with BY4741 *PKH2-GFP*. The SFY95 and SFY96 strains were obtained by crossing BY4741 *VPS27-GFP* (EUROSCARF) with INA106-3D.

The pSF51 and pSF52 plasmids were generated by cloning PCR fragments containing respectively *VPS27* endogenous promoter and *VPS27* gene full length or until nucleotide 1569, amplified from pDL56, between the *Eco*RI and *Bam*HI restriction sites of YCpHAC33. The pDB17 plasmid was generated by cloning a PCR fragment containing the *VPS27* gene amplified from genomic DNA between *Nde*I and *Bam*HI restriction sites of the pET15b plasmid. The pSF55 plasmid bearing the K208R point mutation of Pkh2 was obtained by site-directed mutagenesis of the pRH1250 plasmid using the GGTACGCCGCAAggGTACTAAAC and GTTTAGTACccTTGCGGCGTACC primers. pSF65, pSF66, and pSF69 plasmids bearing the S613A mutation of Vps27 were obtained by site-directed mutagenesis of pSF51, pDB17, and pDL56, respectively, using the GAAAGGCCGCCTgcTCCTCAAGAGG and CCTCTTGAGGAgcAGGCGGCCTTTC primers, whereas pSF68, pSF70, and pSF71 plasmids bearing the S613D mutation were obtained using the GAAAGGCCGCCTgaTCCTCAAGAGG and CCTCTTGAGGAtcAGGCGGCCTTTC primers.

Protein extracts and Western blotting

Cells extracts were prepared by trichloroacetic acid precipitation and NaOH lysis and proteins analyzed by immunoblotting as previously described (Volland *et al*., 1994).

Carboxypeptidase Y secretion assay

A 5-μl drop of culture at OD_{600} of 0.4 was spotted on a YPD plate, left to dry, and then covered with a water-hydrated nitrocellulose membrane (Protran BA85; Whatman, Piscataway, NJ). After 48 h of growth at 30°C the membrane was removed and rinsed with water, and CPY secretion was revealed by immunoblotting with rabbit polyclonal anti-CPY antibodies (a gift from H. Riezman, University of Geneva, Switzerland).

6xHis-tagged protein purification

A 200-ml amount of LB/ampicillin/chloramphenicol was inoculated with BL21 Rosetta (Novagen, Gibbstown, NJ) transformed with pET15b-6His-VPS27. Cells were grown until OD_{600} of 0.5 was reached. Recombinant protein synthesis was induced by addition of 1 mM isopropyl-β-D-thiogalactoside for 2 h at 37°C. Cells were then harvested, snap frozen, and thawed and then resuspended in 2 ml of lysis buffer (50 mM Tris, pH 7.5, 150 mM NaCl, 5 mM imidazole) supplemented with protease inhibitor (Complete Mini-EDTA Free; Roche, Indianapolis, IN). Cells were then lysed by sonication on ice five times for 30 s with 30-s breaks. Insoluble material was removed by centrifugation for 10 min at 13,000 × *g*. Soluble material was loaded on a 500-μl bed volume Ni-Sepharose column (HisTrap HP; GE Healthcare, Piscataway, NJ) equilibrated with lysis buffer. The column was then washed twice with 500 μl of 50 mM imidazole buffer (50 mM Tris, pH 7.5, 150 mM NaCl) and once with 500 μl of 80 mM imidazole buffer. The 6xHis-tagged proteins were eluted by three times 500 μl of 500 mM imidazole buffer. Protein concentration was measured using Bradford reagent (Protein Assay; Bio-Rad, Hercules, CA). The most concentrated fraction was dialyzed overnight against 500 ml of 40 mM 3-(*N*-morpholino)propanesulfonic acid (MOPS)/KOH, pH 7.4, 10 mM $MgCl_2$, and 50% glycerol. Dialyzed proteins were stored at –80°C.

In vitro phosphorylation assay

The *pkh1*Δ strain transformed with empty plasmid (YEp195), YEp195-PKH2-3xHA, or YEp195-$PKH2^{K208R}$-3xHA was grown until exponential phase of growth at 30°C in SC selective medium. The equivalent of 30 OD_{600} units of cells was lysed in 500 μl of lysis buffer (50 mM 4-(2-hydroxyethyl)-1-piperazineethanesulfonic acid, pH7.5, 150 mM KCl, 1 mM EDTA, pH 7.5, 1 mM ethylene glycol tetraacetic acid [EGTA], pH 7.5, 10% glycerol) supplemented with protease inhibitor (Complete Mini-EDTA Free) with 500 μl of glass beads by vortexing for 4 min. The lysate was cleared by two

centrifugations at 500 × *g*. The total lysate protein concentration was quantified by Bradford reagent (Bio-Rad). Volume of total lysate corresponding to 1 mg of proteins was brought up to 900 µl with immunoprecipitation (IP) buffer (50 mM Tris/HCl, pH 7.5, 150 mM NaCl, 1 mM EDTA, pH 7.5, 1 mM EGTA, pH 7.5, 1% Nonidet P-40) supplemented with protease inhibitor (Complete Mini-EDTA Free), and 50 µl of 50% protein G–Sepharose beads (Sigma-Aldrich, St. Louis, MO) and 5 µl of rat anti-HA antibodies (3F10; Roche) were added. The tubes were incubated on an overhead rotator overnight at 4°C. The beads were washed three times with IP buffer and then twice with 40 mM MOPS, pH 7.5.

The beads were then resuspended in 60 µl of phosphorylation buffer (40 mM MOPS, pH 7.5, 10 mM $MgCl_2$, 1 mM dithiothreitol). A 10-µl amount of immune complex beads was mixed with 25 µg of substrate protein in 10 µl of phosphorylation buffer and 2 µl of ATP mix (1 mM ATP, 4 µCi of [γ-^{32}P]ATP). The phosphorylation mixture was incubated for 30 min at room temperature. The reaction was stopped by addition of 4× Laemmli buffer containing 50 mM ATP. The samples were boiled for 5 min and then loaded on a 10% polyacrylamide gel. The gel was treated for 5 min in 12.5% TCA and for 5 min in 50% (vol/vol) EtOH and 10% (vol/vol) acetic acid, dried, and exposed on a phosphoscreen. After 24 h of exposure the screen was scanned using a Typhoon Trio (GE Healthcare).

Subcellular fractionation

The equivalent of 30 OD_{600} units of cells was lysed in 500 µl of phosphate-buffered saline (PBS) and 0.25 M sorbitol supplemented with protease inhibitor (Complete Mini-EDTA Free) with 500 µl of glass beads by vortexing for 4 min at 4°C. The lysate was cleared by two centrifugations of 3 min at 500 × *g*. The cleared lysate was then spun for 10 min at 13,000 × *g*, generating the P13 pellet; the S13 was further spun for 1 h at 100,000 × *g* to generate the P100 and S100. The P13 and P100 were resuspended in the same volume as S100 of PBS, 0.25 M sorbitol, and 1% Triton X-100.

Equal volumes of each fraction were analyzed by SDS–PAGE, followed by immunoblot with mouse monoclonal anti-Vps10 (Invitrogen, Carlsbad, CA), mouse monoclonal anti-HA (Roche), mouse anti-ALP (Invitrogen), mouse anti-Vti1 (a gift from G. F. von Mollard, Universität Bielefeld, Germany), and mouse anti-Pgk1 (Invitrogen) antibodies.

Fluorescence microscopy

Cells expressing the different GFP-tagged proteins were grown to mid-exponential growth phase in selective medium before observation in the selective medium using fluorescence microscopy (Axiovert 200, 100× objective, differential interference contrast and GFP filters [Carl Zeiss, Jena, Germany]). Images were acquired with AxioVision (Zeiss) software using a CoolSnapHQ2 camera (Roper Scientific, Tucson, AZ) and processed with ImageJ software (National Institutes of Health, Bethesda, MD).

ACKNOWLEDGMENTS

We thank Naima Belgareh-Touzé, Scott D. Emr, Rosine Haguenauer-Tsapis, Robert C. Piper, Howard Riezman, and Gabriele Fischer von Mollard for sharing antibodies, strains, and plasmids; J. O. De Craene and N. Joly for critical reading of the manuscript; the Friant laboratory's members for support; and Romeo Ricci for support during the revision process. This work was supported by the Centre National de la Recherche Scientifique (ATIP-CNRS 05-00932 and ATIP-Plus 2008-3098 to S.F.), the Agence Nationale de la Recherche (ANR-07-BLAN-0065 to S.F.), the Fondation Recherche Médicale (FRM INE20051105238 and FRM-Comité Alsace 2006CX67-1 to S.F.), and the Association pour la Recherche sur le Cancer (ARC JR/MLD/MDV-CR306/7901 to S.F.).

REFERENCES

Albuquerque CP, Smolka MB, Payne SH, Bafna V, Eng J, Zhou H (2008). A multidimensional chromatography technology for in-depth phosphoproteome analysis. Mol Cell Proteomics 7, 1389–1396.

Bilodeau PS, Winistorfer SC, Kearney WR, Robertson AD, Piper RC (2003). Vps27-Hse1 and ESCRT-I complexes cooperate to increase efficiency of sorting ubiquitinated proteins at the endosome. J Cell Biol 163, 237–243.

Boura E, Rozycki B, Herrick DZ, Chung HS, Vecer J, Eaton WA, Cafiso DS, Hummer G, Hurley JH (2011). Solution structure of the ESCRT-I complex by small-angle x-ray scattering, EPR, and FRET spectroscopy. Proc Natl Acad Sci USA 108, 9437–9442.

Bugnicourt A, Froissard M, Sereti K, Ulrich HD, Haguenauer-Tsapis R, Galan JM (2004). Antagonistic roles of ESCRT and Vps class C/HOPS complexes in the recycling of yeast membrane proteins. Mol Biol Cell 15, 4203–4214.

Casamayor A, Torrance PD, Kobayashi T, Thorner J, Alessi DR (1999). Functional counterparts of mammalian protein kinases PDK1 and SGK in budding yeast. Curr Biol 9, 186–197.

Chen P, Lee KS, Levin DE (1993). A pair of putative protein kinase genes (YPK1 and YPK2) is required for cell growth in *Saccharomyces cerevisiae*. Mol Gen Genet 236, 443–447.

deHart AK, Schnell JD, Allen DA, Hicke L (2002). The conserved Pkh-Ypk kinase cascade is required for endocytosis in yeast. J Cell Biol 156, 241–248.

Feng Y, Davis NG (2000). Akr1p and the type I casein kinases act prior to the ubiquitination step of yeast endocytosis: Akr1p is required for kinase localization to the plasma membrane. Mol Cell Biol 20, 5350–5359.

Friant S, Lombardi R, Schmelzle T, Hall MN, Riezman H (2001). Sphingoid base signaling via Pkh kinases is required for endocytosis in yeast. EMBO J 20, 6783–6792.

Friant S, Zanolari B, Riezman H (2000). Increased protein kinase or decreased PP2A activity bypasses sphingoid base requirement in endocytosis. EMBO J 19, 2834–2844.

Gietz D, St Jean A, Woods RA, Schiestl RH (1992). Improved method for high efficiency transformation of intact yeast cells. Nucleic Acids Res 20, 1425.

Gill DJ, Teo H, Sun J, Perisic O, Veprintsev DB, Emr SD, Williams RL (2007). Structural insight into the ESCRT-I/-II link and its role in MVB trafficking. EMBO J 26, 600–612.

Gruhler A, Olsen JV, Mohammed S, Mortensen P, Faergeman NJ, Mann M, Jensen ON (2005). Quantitative phosphoproteomics applied to the yeast pheromone signaling pathway. Mol Cell Proteomics 4, 310–327.

Hanafusa H, Ishikawa K, Kedashiro S, Saigo T, Iemura S, Natsume T, Komada M, Shibuya H, Nara A, Matsumoto K (2011). Leucine-rich repeat kinase LRRK1 regulates endosomal trafficking of the EGF receptor. Nat Commun 2, 158.

Hicke L, Zanolari B, Riezman H (1998). Cytoplasmic tail phosphorylation of the alpha-factor receptor is required for its ubiquitination and internalization. J Cell Biol 141, 349–358.

Hierro A, Sun J, Rusnak AS, Kim J, Prag G, Emr SD, Hurley JH (2004). Structure of the ESCRT-II endosomal trafficking complex. Nature 431, 221–225.

Hoeller D *et al.* (2006). Regulation of ubiquitin-binding proteins by monoubiquitination. Nat Cell Biol 8, 163–169.

Hurley JH (2008). ESCRT complexes and the biogenesis of multivesicular bodies. Curr Opin Cell Biol 20, 4–11.

Im YJ, Wollert T, Boura E, Hurley JH (2009). Structure and function of the ESCRT-II-III interface in multivesicular body biogenesis. Dev Cell 17, 234–243.

Inagaki M, Schmelzle T, Yamaguchi K, Irie K, Hall MN, Matsumoto K (1999). PDK1 homologs activate the Pkc1-mitogen-activated protein kinase pathway in yeast. Mol Cell Biol 19, 8344–8352.

Katzmann DJ, Stefan CJ, Babst M, Emr SD (2003). Vps27 recruits ESCRT machinery to endosomes during MVB sorting. J Cell Biol 162, 413–423.

Lata S, Schoehn G, Jain A, Pires R, Piehler J, Gottlinger HG, Weissenhorn W (2008). Helical structures of ESCRT-III are disassembled by VPS4. Science 321, 1354–1357.

Lauwers E, Erpapazoglou Z, Haguenauer-Tsapis R, Andre B (2010). The ubiquitin code of yeast permease trafficking. Trends Cell Biol 20, 196–204.

Marchal C, Dupre S, Urban-Grimal D (2001). Casein kinase I controls a late step in the endocytic trafficking of yeast uracil permease. J Cell Sci 115, 217–226.

Marchal C, Haguenauer-Tsapis R, Urban-Grimal D (1998). A PEST-like sequence mediates phosphorylation and efficient ubiquitination of yeast uracil permease. Mol Cell Biol 18, 314–321.

Marchal C, Haguenauer-Tsapis R, Urban-Grimal D (2000). Casein kinase I-dependent phosphorylation within a PEST sequence and ubiquitination at nearby lysines signal endocytosis of yeast uracil permease. J Biol Chem 275, 23608–23614.

Obita T, Saksena S, Ghazi-Tabatabai S, Gill DJ, Perisic O, Emr SD, Williams RL (2007). Structural basis for selective recognition of ESCRT-III by the AAA ATPase Vps4. Nature 449, 735–739.

Odorizzi G, Babst M, Emr SD (1998). Fab1p PtdIns(3)P 5-kinase function essential for protein sorting in the multivesicular body. Cell 95, 847–858.

Pornillos O, Alam SL, Davis DR, Sundquist WI (2002). Structure of the Tsg101 UEV domain in complex with the PTAP motif of the HIV-1 p6 protein. Nat Struct Biol 9, 812–817.

Reggiori F, Pelham HR (2001). Sorting of proteins into multivesicular bodies: ubiquitin-dependent and -independent targeting. EMBO J 20, 5176–5186.

Ren X, Hurley JH (2011). Structural basis for endosomal recruitment of ESCRT-I by ESCRT-0 in yeast. EMBO J 30, 2130–2139.

Ren X, Kloer DP, Kim YC, Ghirlando R, Saidi LF, Hummer G, Hurley JH (2009). Hybrid structural model of the complete human ESCRT-0 complex. Structure 17, 406–416.

Robinson LC, Menold MM, Garrett S, Culbertson MR (1993). Casein kinase I-like protein kinases encoded by YCK1 and YCK2 are required for yeast morphogenesis. Mol Cell Biol 13, 2870–2881.

Roth AF, Papanayotou I, Davis NG (2011). The yeast kinase Yck2 has a tripartite palmitoylation signal. Mol Biol Cell 22, 2702–2715.

Saksena S, Sun J, Chu T, Emr SD (2007). ESCRTing proteins in the endocytic pathway. Trends Biochem Sci 32, 561–573.

Smolka MB, Albuquerque CP, Chen SH, Zhou H (2007). Proteome-wide identification of in vivo targets of DNA damage checkpoint kinases. Proc Natl Acad Sci USA 104, 10364–10369.

Steen H, Kuster B, Fernandez M, Pandey A, Mann M (2002). Tyrosine phosphorylation mapping of the epidermal growth factor receptor signaling pathway. J Biol Chem 277, 1031–1039.

Stefan CJ, Blumer KJ (1999). A syntaxin homolog encoded by VAM3 mediates down-regulation of a yeast G protein-coupled receptor. J Biol Chem 274, 1835–1841.

Stern KA, Visser Smit GD, Place TL, Winistorfer S, Piper RC, Lill NL (2007). Epidermal growth factor receptor fate is controlled by Hrs tyrosine phosphorylation sites that regulate Hrs degradation. Mol Cell Biol 27, 888–898.

Teo H, Gill DJ, Sun J, Perisic O, Veprintsev DB, Vallis Y, Emr SD, Williams RL (2006). ESCRT-I core and ESCRT-II GLUE domain structures reveal role for GLUE in linking to ESCRT-I and membranes. Cell 125, 99–111.

Urbe S, Mills IG, Stenmark H, Kitamura N, Clague MJ (2000). Endosomal localization and receptor dynamics determine tyrosine phosphorylation of hepatocyte growth factor-regulated tyrosine kinase substrate. Mol Cell Biol 20, 7685–7692.

Volland C, Urban-Grimal D, Geraud G, Haguenauer-Tsapis R (1994). Endocytosis and degradation of the yeast uracil permease under adverse conditions. J Biol Chem 269, 9833–9841.

Williams RL, Urbe S (2007). The emerging shape of the ESCRT machinery. Nat Rev Mol Cell Biol 8, 355–368.

Wollert T, Yang D, Ren X, Lee HH, Im YJ, Hurley JH (2009). The ESCRT machinery at a glance. J Cell Sci 122, 2163–2166.

Zanolari B, Friant S, Funato K, Sutterlin C, Stevenson BJ, Riezman H (2000). Sphingoid base synthesis requirement for endocytosis in *Saccharomyces cerevisiae*. EMBO J 19, 2824–2833.